



Suzuki, H., Harrison, C. J., Shimamura, M., Kohchi, T., & Nishihama, R. (2020). Positional cues regulate dorsal organ formation in the liverwort *Marchantia polymorpha*. *Journal of Plant Research*, 2020. <https://doi.org/10.1007/s10265-020-01180-5>

Peer reviewed version

Link to published version (if available):
[10.1007/s10265-020-01180-5](https://doi.org/10.1007/s10265-020-01180-5)

[Link to publication record in Explore Bristol Research](#)
PDF-document

This is the author accepted manuscript (AAM). The final published version (version of record) is available online via Springer Verlag at <https://doi.org/10.1007/s10265-020-01180-5> . Please refer to any applicable terms of use of the publisher.

University of Bristol - Explore Bristol Research

General rights

This document is made available in accordance with publisher policies. Please cite only the published version using the reference above. Full terms of use are available:
<http://www.bristol.ac.uk/red/research-policy/pure/user-guides/ebr-terms/>

1 Corresponding author: Ryuichi Nishihama

2 Graduate School of Biostudies, Kyoto University, Kyoto 606-8502, Japan

3 Tel: +81-(0)75-753-6390

4 Fax: +81-(0)75-753-6127

5 E-mail: nishihama@lif.kyoto-u.ac.jp

6

7 Membership holders of the Botanical Society of Japan:

8 Masaki Shimamura, Takayuki Kohchi, and Ryuichi Nishihama

9

10 Subject Area:

11 (4) Genetics/Developmental Biology

12

13 Manuscript information:

14 0 table, 7 color figures, 0 black and white figure, 0 supplemental figures, and 0
15 supplemental movie.

16

29 **Abstract**

30 Bryophytes and vascular plants represent the broadest evolutionary divergence in the land
31 plant lineage, and comparative analyses of development spanning this divergence
32 therefore offer opportunities to identify truisms of plant development in general. In
33 vascular plants, organs are formed repetitively around meristems at the growing tips in
34 response to positional cues. In contrast, leaf formation in mosses and leafy liverworts
35 occurs from clonal groups of cells derived from a daughter cell of the apical stem cell
36 known as merophytes, and cell lineage is a crucial factor in repetitive organ formation.
37 However, it remains unclear whether merophyte lineages are a general feature of
38 repetitive organ formation in bryophytes as patterns of organogenesis in thalloid
39 liverworts are unclear. To address this question, we developed a clonal analysis method
40 for use in the thalloid liverwort *Marchantia polymorpha*, involving random low-
41 frequency induction of a constitutively expressed nuclear-targeted fluorescent protein by
42 dual heat-shock and dexamethasone treatment. *M. polymorpha* thalli ultimately derive
43 from stem cells in the apical notch, and the lobes predominantly develop from merophytes
44 cleft to the left and right of the apical cell(s). Sector induction in gemmae and subsequent
45 culture occasionally generated fluorescent sectors that bisected thalli along the midrib and
46 were maintained through several bifurcation events, likely reflecting the border between
47 lateral merophytes. Such thallus-bisecting sectors traversed dorsal air pores and gemma
48 cups, suggesting that these organs arise independently of merophyte cell lineages in
49 response to local positional cues.

50

51 **Keywords (4-6 keywords in alphabetical order)**

52 Apical cell, Cell lineage, Clonal analysis, *Marchantia polymorpha*, Merophyte, Sectors

53

54 **Introduction**

55 Land plant development is characterized by apical growth, in which stem cells residing
56 in the shoot apical meristem produce new tissues and organs, and changes in stem cell
57 and apical function are linked to the origin of three-dimensional land plant forms and their
58 subsequent diversification (reviewed in Harrison 2017; Moody 2020). Whilst bryophyte
59 meristems are thought to have a single apical cell whose geometry and cleavage patterns
60 determine organ position and plants' overall body plan (Harrison et al. 2009; Parihar
61 1967), lycophyte and fern meristems have one to a few apical cells (Harrison and
62 Langdale 2010; Harrison et al. 2007; Sanders et al. 2011), and seed plants have
63 multicellular meristems (Korn 2001, 2002; Poethig 1987; Poethig and Szymkowiak 1995).
64 Apical cell daughters in non-seed plants are called 'merophytes' and proliferate to form
65 clonally related cell groups (Douin 1925; Gifford 1983; Korn 1993). In mosses and leafy
66 liverworts, the apical cells produce merophytes which divide to generate leaves or tissues
67 such as epidermis and parenchyma (Crandall-Stotler 1980; Harrison et al. 2009; Parihar
68 1967; Ruhland 1924). Thus, merophytes serve as a repeating unit of shoot formation, and
69 cell lineage is manifest in organ and tissue development. In contrast to other bryophytes,
70 thalloid liverworts have flattened whole plant bodies in place of forming individual leaves
71 (Crandall-Stotler 1981; Shimamura 2016), and patterns of thallus development and
72 organogenesis are unclear.

73 The liverwort *Marchantia polymorpha* L. grows as a flattened creeping thallus
74 that periodically bifurcates from the apical notch, which houses cuneate apical cell(s) (Fig.
75 1a, b; Shimamura 2016; Solly et al. 2017). The duration between consecutive notch
76 bifurcation events is termed the "plastochron", and plastochron 1 covers the period
77 between gemma germination and the first bifurcation (Fig. 1a; Solly et al. 2017). On the
78 dorsal side of the thallus, an assimilation organ, the 'air chamber' (Fig. 1c), and a cup-
79 shaped organ generating vegetative propagules, the 'gemma cup' (Fig. 1d), respectively
80 develop repetitively or periodically. Histological and anatomical studies have shown that

81 air chamber formation begins with aperture formation at a distance from the apical cells,
82 and then an intercellular space, the ‘air pore’ (Fig. 1b), forms between epidermal cells by
83 cell separation (Fig. 1e; Apostolakos et al. 1982; Ishizaki et al. 2013). Though
84 Apostolakos et al. (1982) concluded from observations of intercellular spaces at the
85 corner of most epidermal cells in *M. paleacea* that air chambers have no distinct mother
86 cell but develop from air pore cells surrounding the initial aperture, direct evidence
87 supporting their conclusion is lacking. In contrast to air pores, gemma cup primordia are
88 evident a few cells away from the apical cells in *M. polymorpha* (Fig. 1f; Barnes and Land
89 1908) suggesting that dorsal merophytes contribute to gemma cup development. Whether
90 dorsal merophytes are the sole contributor, or other merophytes also contribute to gemma
91 cup development is unclear.

92 This lack of clarity around dorsal organogenesis is inherent in histological and
93 anatomical approaches which capture static snapshots of a series of dynamic
94 developmental processes, and the difficulties in distinguishing merophyte borders in fully
95 developed tissues. In this study, we used clonal analysis to label cell lineages (Poethig
96 1987), and found that both air chambers and gemma cups are formed across merophyte
97 boundaries, suggesting that positional cues regulate organogenesis in the liverwort *M.*
98 *polymorpha*.

99

100 **Materials and Methods**

101 **Plant materials and growth condition**

102 Male accessions of *M. polymorpha*, Takaragaike-1 (Tak-1) were used as wild-type plants.
103 *M. polymorpha* was cultured on half strength Gamborg’s B5 medium containing 1% agar
104 under 50-60 $\mu\text{mol photon m}^{-2} \text{s}^{-1}$ continuous white fluorescent light at 22 °C.

105

106 **Plasmid construction and transformation**

107 Plasmid pMpGWB337tdTN-GUS was generated by LR recombination between

108 pMpGWB337tdTN (Sugano et al. 2018) and pENTR-gus (Thermo Fisher Scientific,
109 Waltham, MA, USA) using LR Clonase II (Thermo Fisher Scientific) and used for
110 *Agrobacterium*-mediated transformation of Tak-1 thallus (Kubota et al. 2013).
111 *proMpSYP13B:mTurquoise2-MpSYP13B* vector was generated as described in Kanazawa
112 et al. (2016). An mTurquoise2-coding sequence was amplified with a primer set,
113 mTurquoise2_BamHI_IF_Fw
114 (CCCCTTCACCGGATCATGGTGTCTAAGGGTGAGGAAC) and
115 mTurquoise2_BamHI_IF_Rv
116 (GCTGCCCGCCGGATCCTTTGTAAAGCTCATCCATTCCG), and then inserted into
117 the BamHI-digested *proMpSYP13B:MpSYP13B* entry vector (Kanazawa et al. 2016)
118 using In-Fusion HD Cloning System (TaKaRa, Shiga, Japan). The resultant entry vector
119 was then introduced into pMpGWB101 (Ishizaki et al. 2015) by LR recombination, and
120 then used for *Agrobacterium*-mediated transformation of pMpGWB337tdTN-GUS plant
121 thallus (Kubota et al. 2013).

122

123 **SEM imaging**

124 SEM images were taken with 21-day-old Tak-1 thalli using TM3000 (Hitachi High
125 Technologies, Tokyo, Japan).

126

127 **Clonal analysis and fluorescence observation**

128 Cre induction on mature gemmae was performed as follows: gemmae on a plate were
129 treated with 3 μ L of a solution containing 5 μ M DEX, air dried for 10 to 20 minutes, and
130 subjected to heat shock by incubating the plate in a 37 °C air incubator for various periods.

131 Cre induction on thalli was performed as follows: 8-day-old thalli were vacuum-
132 infiltrated in a solution containing 5 μ M DEX, transplanted onto agar media, air dried for
133 10 to 20 minutes, and then heat-shocked in a 37 °C incubator for 35 to 50 minutes.

134 Sector-formed thalli were embedded in 6% agar block and sectioned into ~200-

135 μm -thick slices with LinearSlicer Pro 7(DOSAKA EM, Kyoto, Japan). tdTomato,
136 mTurquoise2, and bright field images in mature gemmae, 1-day-old gemmalings, 6-day-
137 old thalli, and sliced samples were captured with fluorescence microscope BZ-X710
138 (Keyence, Osaka, Japan) and merged after equal adjustment of contrast and brightness
139 for visibility by the BZ-X Analyzer (Keyence). Thalli were observed with fluorescence
140 dissection microscope Leica M205 C (Leica, Wetzlar, Germany). Obtained images were
141 manually merged by using ImageJ (<https://imagej.nih.gov/ij/>) after contrast and
142 brightness were adjusted for visibility. Contribution of tdTomato-positive and -negative
143 regions to a gemma cup was evaluated by counting the number of serrations existing in
144 each region.

145

146 **Histochemical assay for GUS activity**

147 Histochemical assay for GUS activity was performed as described previously (Ishizaki et
148 al. 2012).

149

150 **Results**

151 **Exploitation of clonal analysis system**

152 To determine how dorsal structures develop, we first established a Cre-*loxP* based clonal
153 sector induction system (Fig. 2a). A construct was designed to constitutively express a
154 floxed β -glucuronidase (*GUS*) gene under the *M. polymorpha* *EF1 α* promoter
155 (*proMpEF1 α*), and conditionally express a Cre-recombinase/gluocorticoid receptor (GR)
156 fusion protein under a *M. polymorpha* heat-shock promoter, *MpHSP17.8A1* (Fig. 2a;
157 Nishihama et al. 2016). The rationale for sector induction was that, following heat shock
158 and dexamethasone (DEX) treatment, the Cre protein would excise the *GUS* gene
159 allowing expression of a nuclear targeted red fluorescent protein, tdTomato-NLS, under
160 *proMpEF1 α* (Sugano et al. 2018). Two elements to control conditional expression of the
161 *Cre* gene were included to avoid leaky excision of the floxed region. This system was

162 expected to mark clonal sectors negatively by the absence of GUS staining or positively
163 by the presence of red fluorescent signal (Fig. 2b).

164 Clonal analysis requires the production of many sectors induced randomly at
165 different stages of development, and there is therefore an optimal frequency of sector
166 induction. Whereas a low frequency of induction generates too few sectors to generate
167 sufficient data for analysis, a high frequency of induction can induce overlapping sectors,
168 becoming uninformative. To optimise the frequency of sector induction and analyse
169 organogenesis in gemmalings and thalli, we first treated gemmae with a solvent control
170 solution or a solution containing 5 μ M DEX, and then heat-shocked gemmae for different
171 periods of time at 37 °C. We subsequently examined gemmae by fluorescence
172 microscopy. The frequency of cells showing fluorescence in the gemma increased as the
173 duration of the heat-shock increased in DEX-treated gemmae, but increased to a lesser
174 extent in untreated gemmae such that sectors were absent in gemmae with no heat shock
175 and present in almost all cells in gemmae that were heat-shocked for 80 minutes (Fig. 2c).
176 A 30-40 minute heat-shock induced sectors at a moderate frequency that was compatible
177 with the requirements of clonal analysis, and was thus used in further experiments, unless
178 otherwise noted.

179

180 **Lateral merophytes bisect thallus lobes**

181 Cre induction in mature gemmae and subsequent plant development caused sector
182 formation in various patterns. Some sectors bisected the thallus lobe (Fig. 3), spanning
183 the dorsal to ventral axis (Fig. 3a), and such sectors persisted through several bifurcation
184 events with well-defined sharp borders (Fig. 3b), consistent with a lateral merophyte
185 origin (see merophyte sectors in Harrison et al. 2007; Harrison et al. 2009; Sanders et al.
186 2011 for comparison).

187

188 **Air pores are formed independently of merophyte cell lineage**

189 Observations of air chambers at sector junctions showed an overlap with the edge of some
190 air chambers, but other air chambers were divided into fluorescence-positive and -
191 negative regions (Fig. 4a). Whilst the former constituted approximately half of cases,
192 amongst the latter, a pattern where the sector border was positioned in the centre of the
193 air pore predominated, but in some cases sectors were off centre (Fig. 4b). Only small
194 proportion of air chambers had sectors that did not cross the air pore (Fig. 4b).
195 Observation in an early developmental stage revealed sectors that covered not only entire
196 air chambers but also half air chambers with the sector border positioned in the centre of
197 the air pore (Fig. 4c). These data suggest that air chambers can be formed either within a
198 merophyte cell lineage or between merophyte cell lineages (see Fig. 7).

199

200 **Gemma cups are a multi-lineage-comprised organ**

201 Next, we observed gemma cups that had formed during the second to fourth plastochrons
202 (Fig. 5a; Solly et al. 2017) on thalli with persistent bisecting sectors (Fig. 3b) and found
203 that such gemma cups were also bisected by the sectors and sometimes contained both
204 fluorescence-positive and -negative gemmae (Fig. 5b). Not only the wall, but also the
205 floor of gemma cups (where gemma initials arise) were separated by such sectors (Fig.
206 5c). These results suggest that gemma cups are not derived from a single merophyte, but
207 multiple merophytes. Contribution of a fluorescence-positive region (or conversely a
208 fluorescence-negative region) to a gemma cup varied depending on the timing of its
209 formation relative to notch bifurcation; those formed during the second and fourth
210 plastochrons showed a range of contributions from 0 to 100%, while those formed during
211 the third plastochron showed approximately 50% contribution (Fig. 5d). These results
212 suggest that gemma cups initiate from two or more cells at the boundary between thallus
213 lobes arising from lateral merophytes, that the process of bifurcation has some inherent
214 variability, and that positional cues are important in gemma cup development.

215 Gemma cup initials are first recognizable a few cells away from the apical cells
216 (Barnes and Land 1908), and the dorsal merophyte is believed to participate in gemma
217 cup development. However, this idea has never been demonstrated experimentally.
218 Because gemma cups are never formed during the first plastochron (Fig. 5a), we induced
219 Cre-*loxP* recombination on 8-day-old thalli, during the second plastochron. Sectors that
220 were several cells wide emerged along the midrib during the third plastochron. These
221 line-shaped sectors were later separated from the apical notches (Fig. 6a), and were only
222 present on the dorsal surface (Fig. 6b), suggesting a dorsal merophyte origin. Such sectors
223 also overlapped with gemma cups (Fig. 6c), suggesting a minor contribution of dorsal
224 merophytes to gemma cup development. Taken together, these observations suggest that
225 gemma cups arise from dorsal merophytes and dorsal derivatives of lateral merophytes
226 (Fig. 7).

227

228 **Discussion**

229 Clonal analysis has considerably contributed to understanding plant development.
230 Methodologies for clonal analysis widely vary, involving ploidy changes induced by
231 colchicine (Satina et al. 1940), activation of *GUS* transgene expression by random or heat-
232 shock-mediated removal of transposons (Dolan et al. 1994; Kidner et al. 2000; Scheres et
233 al. 1994), inactivation of *GUS* transgene expression by heat-shock-mediated Cre-*loxP*
234 excision (Saulsberry et al. 2002), pale green pigmentation or chloroplast biogenesis
235 defects induced by X-ray irradiation (Harrison et al. 2007; Harrison et al. 2009),
236 utilisation of variegated species (Sanders et al. 2011), and so on. This paper reports a new
237 clonal analysis method for *M. polymorpha*, which we anticipate will contribute to
238 understanding patterns of *M. polymorpha* development. For the purpose of lineage
239 visualisation, our method could be further improved by incorporating a multi-colour
240 system such as Brainbow (Livet et al. 2007) and Brother of Brainbow (Wachsman et al.
241 2011). Clonal analysis could be utilised to analyse gene functions in the context of

242 specific cell lineages or positions (Heidstra et al. 2004; Sieburth et al. 1998). By taking
243 advantage of live imaging, our method could be widely applied to conditional genetic
244 analyses using various molecular tools established in *M. polymorpha* (Ishizaki et al. 2015;
245 Kopischke et al. 2017; Mano et al. 2018; Nishihama et al. 2016; Sugano et al. 2018).

246 Here, Cre induction in mature gemmae and subsequent growth occasionally
247 generated sectors that bisected thalli and were maintained through bifurcation events, and
248 such sectors are likely to arise by Cre induction in lateral merophytes or apical cells. Some
249 air pores on such sectors were divided into fluorescence-positive and -negative regions
250 (Fig. 4). Air chambers are known to arise from initial apertures that are formed in the
251 limited area around an apical cell, and aperture-surrounding cells later develop into air
252 pores (Apostolakos et al. 1982). Our analysis demonstrated that air pores could emerge
253 across merophyte boundaries as well as within single merophytes, suggesting that air pore
254 formation does not depend on cell lineages but on local cues around the notch (Fig. 7).
255 We further found that most air-chamber sectors traversed air pores, suggesting that cells
256 that constitute air chambers are derived from initial aperture-surrounding cells, which is
257 consistent with the conclusions by Apostolakos et al. (1982).

258 Gemma cups were also divided by thallus-bisecting sectors (Fig. 5), suggesting
259 that no single initial cell gives rise to gemma cups and that gemma cup development is
260 controlled by local cues. Our observations that the boundary of thallus-bisecting sectors
261 represents the border of lateral merophytes and that dorsal merophyte sectors are
262 incorporated into gemma cups (Fig. 6) demonstrate that gemma cups derive from both
263 dorsal and lateral merophytes (Fig. 7). Though the mechanisms that allow lateral
264 merophytes to contribute differentially to gemma cup formation (Fig. 5d) are unclear, the
265 degree of lateral proliferation of lateral and dorsal merophyte cells may vary depending
266 on the plastochron, or due to plasticity. Recently, an R2R3-type MYB transcription factor,
267 GEMMA CUP-ASSOCIATED MYB1 (GCAM1), was reported to play an essential role
268 in gemma cup formation (Yasui et al. 2019). *GCAM1* is expressed in the notch and the

269 gemma cup floor and is proposed to maintain dorsal cells near the apical cell in
270 undifferentiated status for gemma cup formation (Yasui et al. 2019). Clarification of the
271 early expression pattern of *GCAMI* in relation to dorsal and lateral merophytes could
272 provide clues to the mechanism of gemma cup formation.

273 In angiosperms, tissue and organ differentiation is based on cell fates that are
274 determined by positional signals (Kidner et al. 2000; Reinhardt et al. 2005; Scheres 2001;
275 Scheres et al. 1994; Sussex 1951, 1954; van den Berg et al. 1995). Flow of the
276 phytohormone auxin specifies the site of cell differentiation for organ formation, such as
277 leaves and lateral roots. Cell lineages also contribute to the formation of tissue layers,
278 such as the tunica and corpus layers of the shoot apical meristem and the radial layers of
279 root tissues, but their identities are often specified by cell-cell communications with other
280 lineage cells. In *M. polymorpha*, auxin signaling via transcriptional regulation plays
281 critical roles in the development of gemmae through regulation of cell division patterns
282 (Kato et al. 2017). The intermerophyte pattern of organogenesis revealed in this study
283 suggests that similar local signal-mediated cell-fate determination operates in *M.*
284 *polymorpha*. In contrast, lateral organs in leafy bryophytes arise from merophyte cell
285 lineages with clear histological boundaries (Crandall-Stotler 1980; Harrison et al. 2009;
286 Parihar 1967; Ruhland 1924). Changes in the cell fate determination system may have led
287 to the morphological diversification of complex thalloid liverworts.

288

289 **Acknowledgements**

290 We thank Takashi Ueda and Takehiko Kanazawa for kindly providing the Mp*SYP13B*
291 entry vector. We thank Shohei Yamaoka, Sakiko Ishida, Akari Ito, Moe Kagao, Masaya
292 Tsumura, Runa Sato and Yuki Sato for helpful discussion. This work was supported by
293 the Japan Society for the Promotion of Science KAKENHI (grant number JP18J12698 to
294 H.S.), the Ministry of Education, Culture, Sports, Science & Technology KAKENHI
295 (grant number 18H04836 to R.N.), and SPIRITS 2017 of Kyoto University to R.N.

296 **References**

- 297 Apostolakos P, Galatis B, Mitrakos K (1982) Studies on the development of the air pores
298 and air chambers of *Marchantia paleacea*. 1. Light microscopy. *Ann Bot* 49:377-396
- 299 Barnes CR, Land WJG (1907) Bryological papers. I. The origin of air chambers. *Bot Gaz*
300 44:197-213
- 301 Barnes CR, Land WJG (1908) Bryological papers. II. The origin of the cupule of
302 *Marchantia*. *Bot Gaz* 46:401-409
- 303 Crandall-Stotler B (1980) Morphogenetic designs and a theory of bryophyte origins and
304 divergence. *BioScience* 30:580-585
- 305 Crandall-Stotler B (1981) Morphology/anatomy of hepatics and anthocerototes. J. Cramer,
306 Vaduz, Lichtenstein
- 307 Dolan L, Duckett CM, Grierson C, Linstead P, Schneider K, Lawson E, Dean C, Poethig
308 S, Roberts K (1994) Clonal relationships and cell patterning in the root epidermis of
309 *Arabidopsis*. *Development* 120:2465-2474
- 310 Douin C (1925) La théorie des initiales chez les Hépatiques à feuilles. *Bull Soc Bot Fr*
311 72:565-591
- 312 Gifford EMJ (1983) Concept of apical cells in bryophytes and pteridophytes. *Ann Rev*
313 *Plant Physiol* 34:419-440
- 314 Harrison CJ (2017) Development and genetics in the evolution of land plant body plans.
315 *Phil Trans R Soc B* 372:20150490
- 316 Harrison CJ, Langdale JA (2010) Comment: The developmental pattern of shoot apices
317 in *Selaginella kraussiana* (Kunze) A. Braun. *Int J Plant Sci* 171:690-692
- 318 Harrison CJ, Rezvani M, Langdale JA (2007) Growth from two transient apical initials in
319 the meristem of *Selaginella kraussiana*. *Development* 134:881-889
- 320 Harrison CJ, Roeder AH, Meyerowitz EM, Langdale JA (2009) Local cues and
321 asymmetric cell divisions underpin body plan transitions in the moss *Physcomitrella*
322 *patens*. *Curr Biol* 19:461-471
- 323 Heidstra R, Welch D, Scheres B (2004) Mosaic analyses using marked activation and

- 324 deletion clones dissect *Arabidopsis* SCARECROW action in asymmetric cell division.
325 Genes Develop 18:1964-1969
- 326 Ishizaki K, Mizutani M, Shimamura M, Masuda A, Nishihama R, Kohchi T (2013)
327 Essential role of the E3 ubiquitin ligase NOPPERABO1 in schizogenous intercellular
328 space formation in the liverwort *Marchantia polymorpha*. Plant Cell 25:4075-4084
- 329 Ishizaki K, Nishihama R, Ueda M, Inoue K, Ishida S, Nishimura Y, Shikanai T, Kohchi T
330 (2015) Development of Gateway binary vector series with four different selection
331 markers for the liverwort *Marchantia polymorpha*. PLOS ONE 10:e0138876
- 332 Ishizaki K, Nonomura M, Kato H, Yamato KT, Kohchi T (2012) Visualization of auxin-
333 mediated transcriptional activation using a common auxin-responsive reporter system in
334 the liverwort *Marchantia polymorpha*. J Plant Res 125:643-651
- 335 Kanazawa T, Era A, Minamino N, Shikano Y, Fujimoto M, Uemura T, Nishihama R,
336 Yamato KT, Ishizaki K, Nishiyama T, Kohchi T, Nakano A, Ueda T (2016) SNARE
337 molecules in *Marchantia polymorpha*: unique and conserved features of the membrane
338 fusion machinery. Plant Cell Physiol 57:307-324
- 339 Kato H, Kouno M, Takeda M, Suzuki H, Ishizaki K, Nishihama R, Kohchi T (2017) The
340 roles of the sole activator-type auxin response factor in pattern formation of *Marchantia*
341 *polymorpha*. Plant Cell Physiol 58:1642-1651
- 342 Kidner C, Sundaresan V, Roberts K, Dolan L (2000) Clonal analysis of the *Arabidopsis*
343 root confirms that position, not lineage, determines cell fate. Planta 211:191-199
- 344 Kopischke S, Schussler E, Althoff F, Zachgo S (2017) TALEN-mediated genome-editing
345 approaches in the liverwort *Marchantia polymorpha* yield high efficiencies for targeted
346 mutagenesis. Plant Methods 13:20
- 347 Korn RW (1993) Apical cells as meristems. Acta Biotheor 41:175-189
- 348 Korn RW (2001) Analysis of shoot apical organization in six species of the Cupressaceae
349 based on chimeric behavior. Am J Bot 88:1945-1952
- 350 Korn RW (2002) Chimeric patterns in *Juniperus chinensis* 'Torulosa Variegata'
351 (Cupressaceae) expressed during leaf and stem formation. Am J Bot 89:758-765
- 352 Kubota A, Ishizaki K, Hosaka M, Kohchi T (2013) Efficient *Agrobacterium*-mediated

353 transformation of the liverwort *Marchantia polymorpha* using regenerating thalli. Biosci
354 Biotechnol Biochem 77:167-172

355 Livet J, Weissman TA, Kang H, Draft RW, Lu J, Bennis RA, Sanes JR, Lichtman JW
356 (2007) Transgenic strategies for combinatorial expression of fluorescent proteins in the
357 nervous system. Nature 450:56-62

358 Mano S, Nishihama R, Ishida S, Hikino K, Kondo M, Nishimura M, Yamato KT, Kohchi
359 T, Nakagawa T (2018) Novel gateway binary vectors for rapid tripartite DNA assembly
360 and promoter analysis with various reporters and tags in the liverwort *Marchantia*
361 *polymorpha*. PLOS ONE 13:e0204964

362 Moody L (2020) Three-dimensional growth: A developmental innovation that facilitated
363 plant terrestrialization. J Plant Res. <https://doi.org/10.1007/s10265-020-01173-4>

364 Nishihama R, Ishida S, Urawa H, Kamei Y, Kohchi T (2016) Conditional gene
365 expression/deletion systems for *Marchantia polymorpha* using its own heat-shock
366 promoter and Cre/loxP-mediated site-specific recombination. Plant Cell Physiol 57:271-
367 280

368 Parihar NS (1967) An introduction to Embryophyta volume I: Bryophyta. Indian
369 Universities Press, Allahbad

370 Poethig RS (1987) Clonal analysis of cell lineage patterns in plant development. Am J
371 Bot 74:581-594

372 Poethig RS, Szymkowiak EJ (1995) Clonal analysis of leaf development in maize.
373 Maydica (Italy) 40:67-76

374 Reinhardt D, Frenz M, Mandel T, Kuhlemeier C (2005) Microsurgical and laser ablation
375 analysis of leaf positioning and dorsoventral patterning in tomato. Development 132:15-
376 26

377 Ruhland W (1924) Musci. Allgemeiner Teil. Verlag von Wilhelm Engelmann, Leipzig

378 Sanders HL, Darrah PR, Langdale JA (2011) Sector analysis and predictive modelling
379 reveal iterative shoot-like development in fern fronds. Development 138:2925-2934

380 Satina S, Blakeslee AF, Avery AG (1940) Demonstration of the three germ layers in the
381 shoot apex of datura by means of induced polyploidy in periclinal chimeras. Am J Bot

382 27:895-905

383 Saulsberry A, Martin PR, O'Brien T, Sieburth LE, Pickett FB (2002) The induced sector
384 *Arabidopsis* apical embryonic fate map. *Development* 129:3403-3410

385 Scheres B (2001) Plant Cell Identity. The role of position and lineage. *Plant Physiol*
386 125:112-114

387 Scheres B, Wolkenfelt H, Willemsen V, Terlouw M, Lawson E, Dean C, Weisbeek P
388 (1994) Embryonic origin of the *Arabidopsis* primary root and root meristem initials.
389 *Development* 120:2475-2487

390 Shimamura M (2016) *Marchantia polymorpha*: taxonomy, phylogeny and morphology of
391 a model system. *Plant Cell Physiol* 57:230-256

392 Sieburth LE, Drews GN, Meyerowitz EM (1998) Non-autonomy of *AGAMOUS* function
393 in flower development: use of a *Cre/loxP* method for mosaic analysis in *Arabidopsis*.
394 *Development* 125:4303

395 Solly JE, Cunniffe NJ, Harrison CJ (2017) Regional growth rate differences specified by
396 apical notch activities regulate liverwort thallus shape. *Curr Biol* 27:16-26

397 Sugano SS, Nishihama R, Shirakawa M, Takagi J, Matsuda Y, Ishida S, Shimada T, Hara-
398 Nishimura I, Osakabe K, Kohchi T (2018) Efficient CRISPR/Cas9-based genome editing
399 and its application to conditional genetic analysis in *Marchantia polymorpha*. *PLOS ONE*
400 13:e0205117

401 Sussex IM (1951) Experiments on the cause of dorsiventrality in leaves. *Nature* 167:651-
402 652

403 Sussex IM (1954) Experiments on the cause of dorsiventrality in leaves. *Nature* 174:351-
404 352

405 van den Berg C, Willemsen V, Hage W, Weisbeek P, Scheres B (1995) Cell fate in the
406 *Arabidopsis* root meristem determined by directional signalling. *Nature* 378:62-65

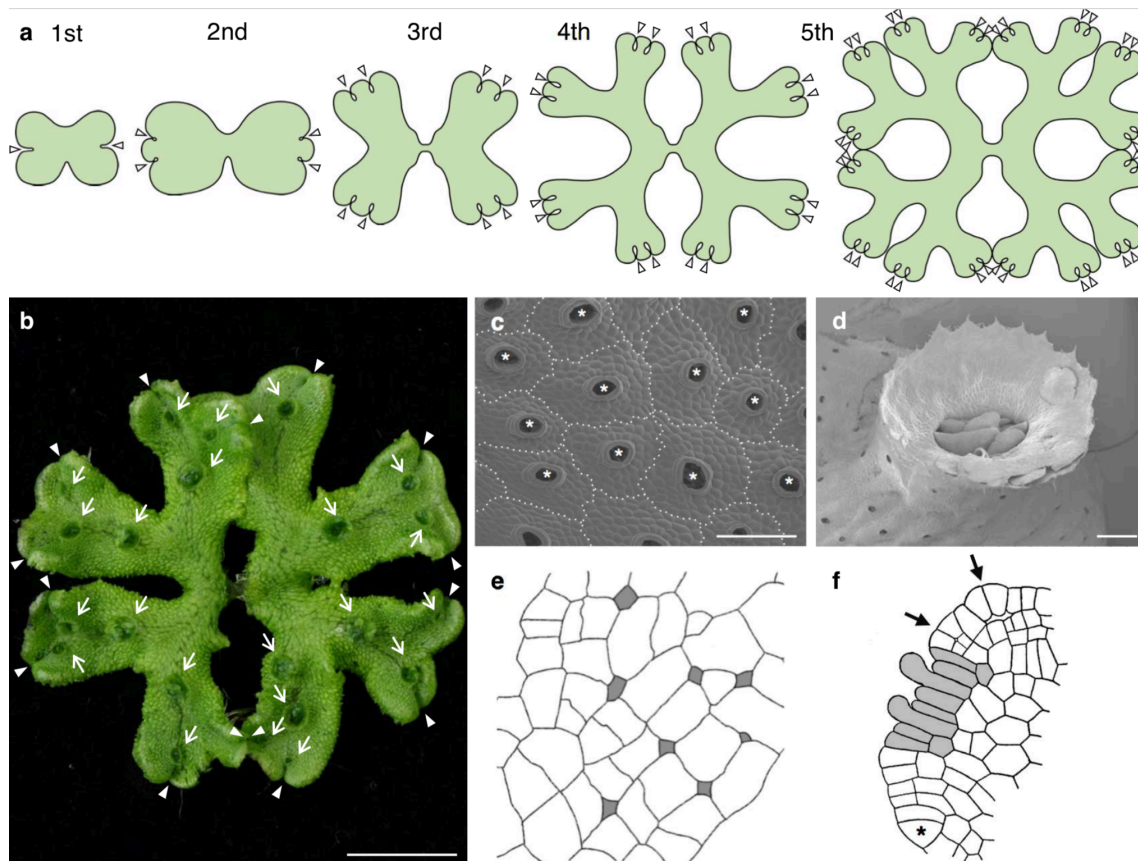
407 Wachsman G, Heidstra R, Scheres B (2011) Distinct cell-autonomous functions of
408 *RETINOBLASTOMA-RELATED* in *Arabidopsis* stem cells revealed by the Brother of
409 Brainbow clonal analysis system. *Plant Cell* 23:2581-2591

410 Yasui Y, Tsukamoto S, Sugaya T, Nishihama R, Wang Q, Kato H, Yamato KT, Fukaki H,
411 Mimura T, Kubo H, Theres K, Kohchi T, Ishizaki K (2019) GEMMA CUP-
412 ASSOCIATED MYB1, an ortholog of axillary meristem regulators, is essential in
413 vegetative reproduction in *Marchantia polymorpha*. *Curr Biol* 29:3987-3995

414

415 **Figures and Figure legends**

416



417

418 **Fig. 1** Notch bifurcations and dorsal structures of the thallus of *M. polymorpha*.

419 **a** Scheme of bifurcating thalli in the n th plastochron stages with exponentially increasing

420 apical notches. Arrowheads indicate apical notches. **b** A 21-day-old *M. polymorpha*

421 thallus in the 4th plastochron. Arrows and Arrowheads indicate gemma cups and apical

422 notches, respectively. Scale bar = 5 mm. **c** Scanning electron microscope (SEM) image

423 of air chambers with one air pore each. Dotted lines and asterisks indicate border of air

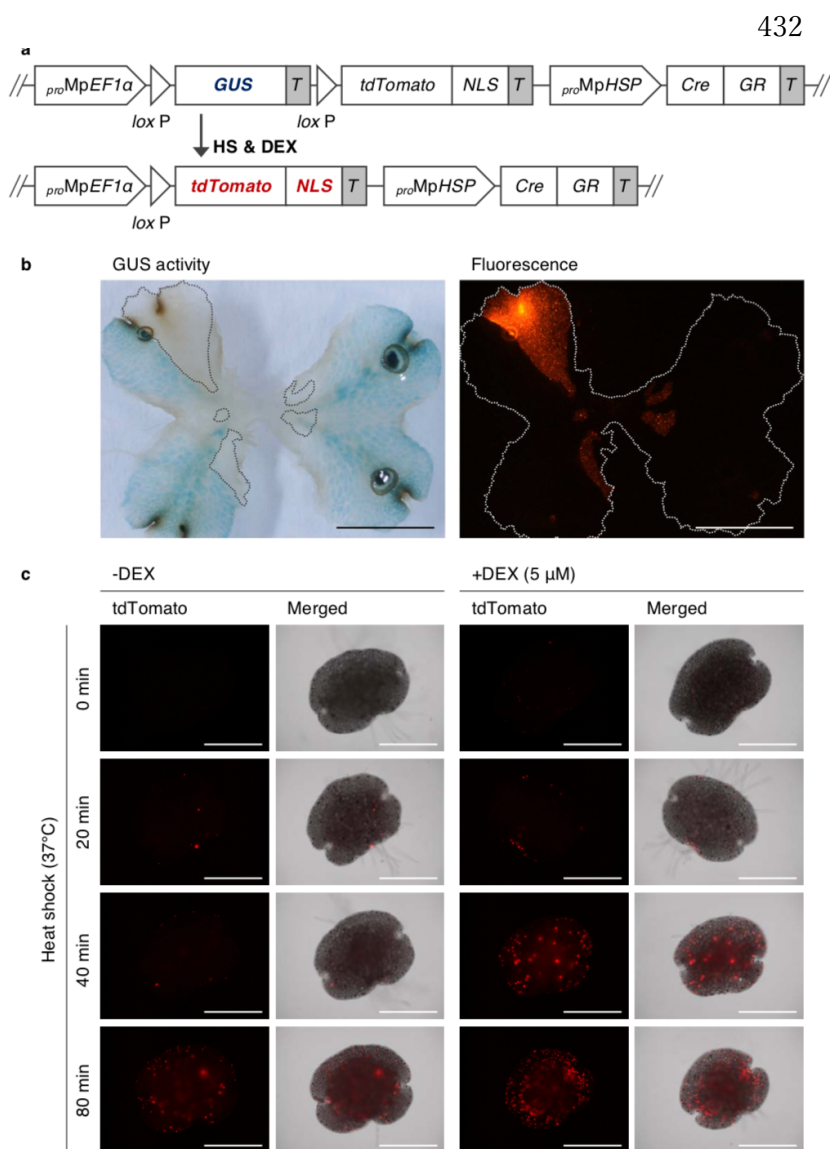
424 chambers and air pores, respectively. Scale bar = 200 μ m. **d** SEM image of a gemma cup

425 with serrated edges. Scale bar = 500 μ m. **e** Surface view of initial apertures (grey) which

426 develop into an air pore (Redrawn from Apostolakos et al. (1982)). **f** Vertical longitudinal

427 view of the apical cell and its derivatives. An asterisk, grey area, arrows indicate an apical

428 cell, gemma cup initial region, young air chambers, respectively (Redrawn from Barnes
 429 and Land (1908)). It should be noted that Barnes and Land proposed that initiation of air
 430 chambers occurs internally at the intersection of daughter cells from a single mother cell
 431 (Barnes and Land 1907), and that the present picture is drawn as such.

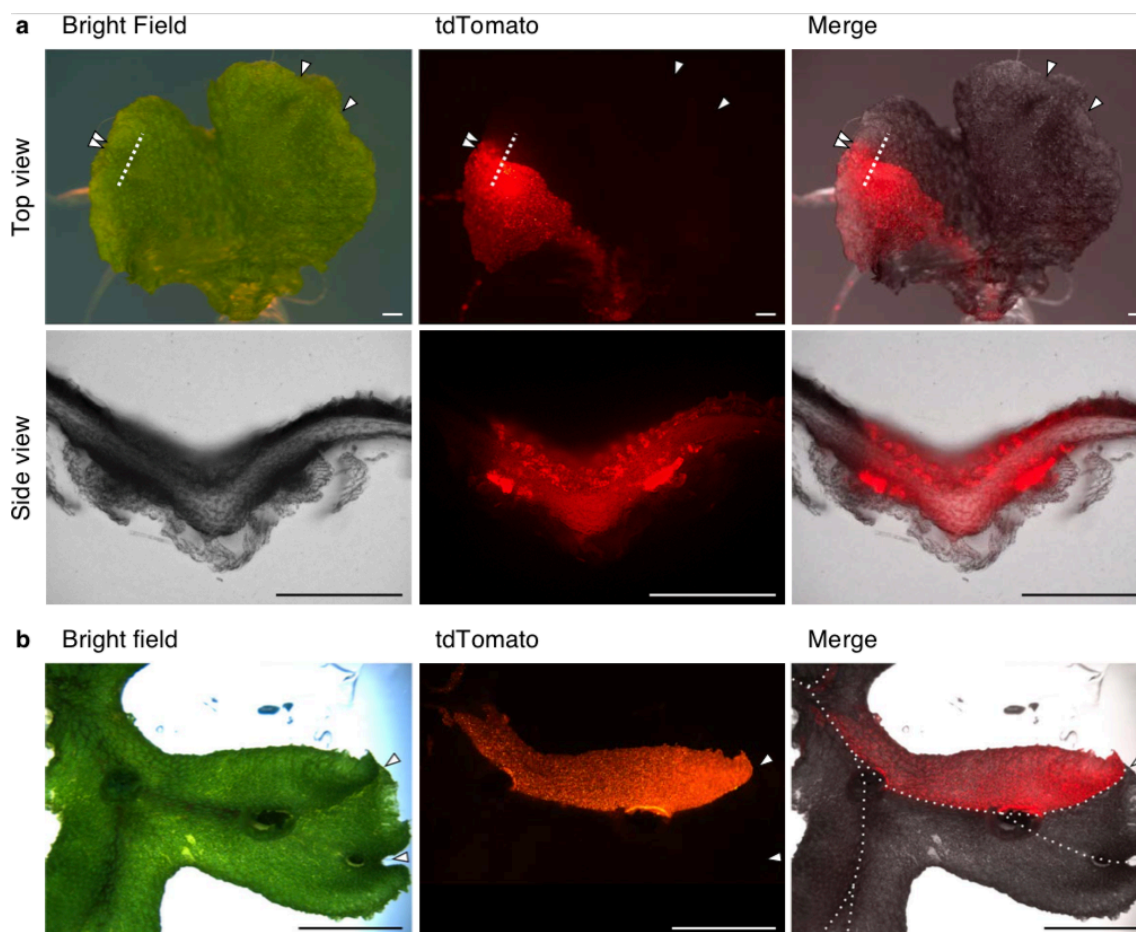


451 **Fig. 2** Clonal analysis system in *M. polymorpha*.

452 **a** Schematic diagram of the construct used in clonal analysis. In the standard state (top),
 453 *tdTomato-NLS* is not transcribed due to an upstream terminator. Heat shock (HS) and
 454 dexamethasone (DEX) treatments induce Cre-*loxP*-mediated excision of the *loxP*-

455 flanked region (bottom), which in turn constitutively switches on *tdTomato-NLS*. *T*:
 456 *NOS* terminator. **b** Reciprocal formation of GUS and tdTomato sectors. This plant was
 457 treated with HS and DEX in mature gemmae and grown for 14 days. Grey dotted lines
 458 on the left panel indicates approximate position of tdTomato-positive sectors. A white
 459 dotted line on the right panel indicate an outline of the thallus. Bars = 5 mm. **c**
 460 Efficiency of Cre-*loxP* recombination. Mature gemmae of the transgenic line were
 461 treated with or without DEX, and then heat-shocked for 0, 20, 40, or 80 min in a 37 °C
 462 incubator. One day after the induction, the plants showed fluorescence in a HS- and
 463 DEX-dependent manner. Scale bars = 500 μm.

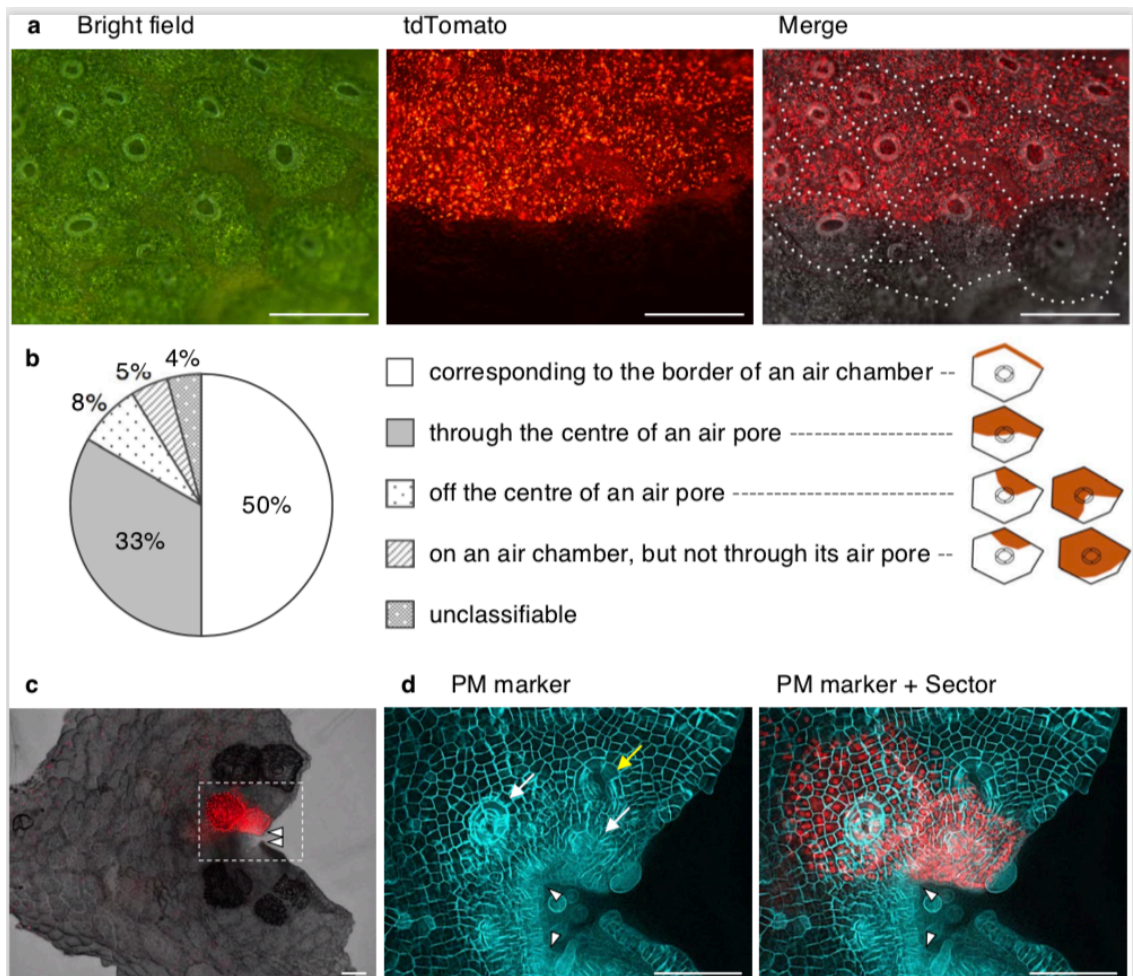
464



465

466 **Fig. 3** Sectors that bisect thallus lobes

467 **a** Top (upper row) and side (lower row) view of a sector bisecting a thallus lobe in the
 468 third plastochron of a 13-day-old plant. Dotted lines indicate the approximate position of
 469 the side-view section (basal side observed). Arrowheads indicate apical notches. Scale
 470 bars = 500 μm . **b** A sector bisecting a thallus lobe from the base to an apical notch in the
 471 fourth plastochron of a 23-day-old plant. Dotted lines indicate midribs. Arrows and
 472 arrowheads indicate gemma cups and apical notches, respectively. Scale bar = 5 mm.



473

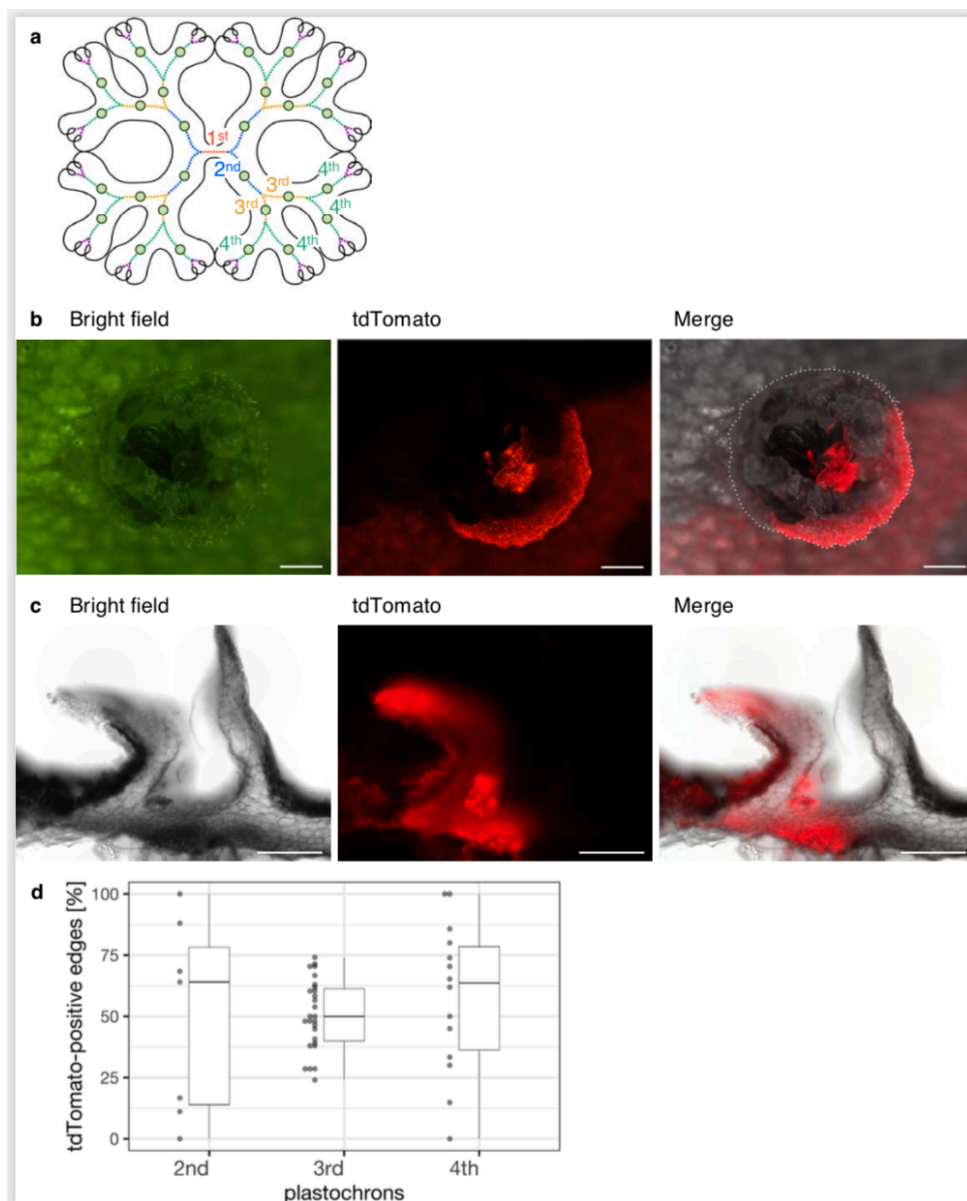
474 **Fig. 4** Division of air pores and air chambers by thallus-bisecting sectors

475 **a** A tdTomato-positive sector on dorsal surface of a thallus. Dotted lines in the merged
 476 picture indicate the edges of air chambers. Scale bars = 500 μm . **b** Ratio of relative
 477 position of sectors to an air pores (see graph legends and schematic illustrations). $n = 192$

478 air pores from 10 merophyte sectors. **c, d** A notch-adjacent sector in the second
 479 plastochron of a 6-day-old plant (**c**) and its magnified view around the notch within the
 480 white dotted rectangle (**d**). As a plasma membrane (PM) marker, mTurquoise2-tagged
 481 MpSYP13B (Kanazawa et al. 2016) was co-expressed under the regulation of its native
 482 promoter. Arrowheads indicate apical notches. White and yellow arrows indicate air pores
 483 formed within and across a sectorized region, respectively. Scale bars = 100 μ m.

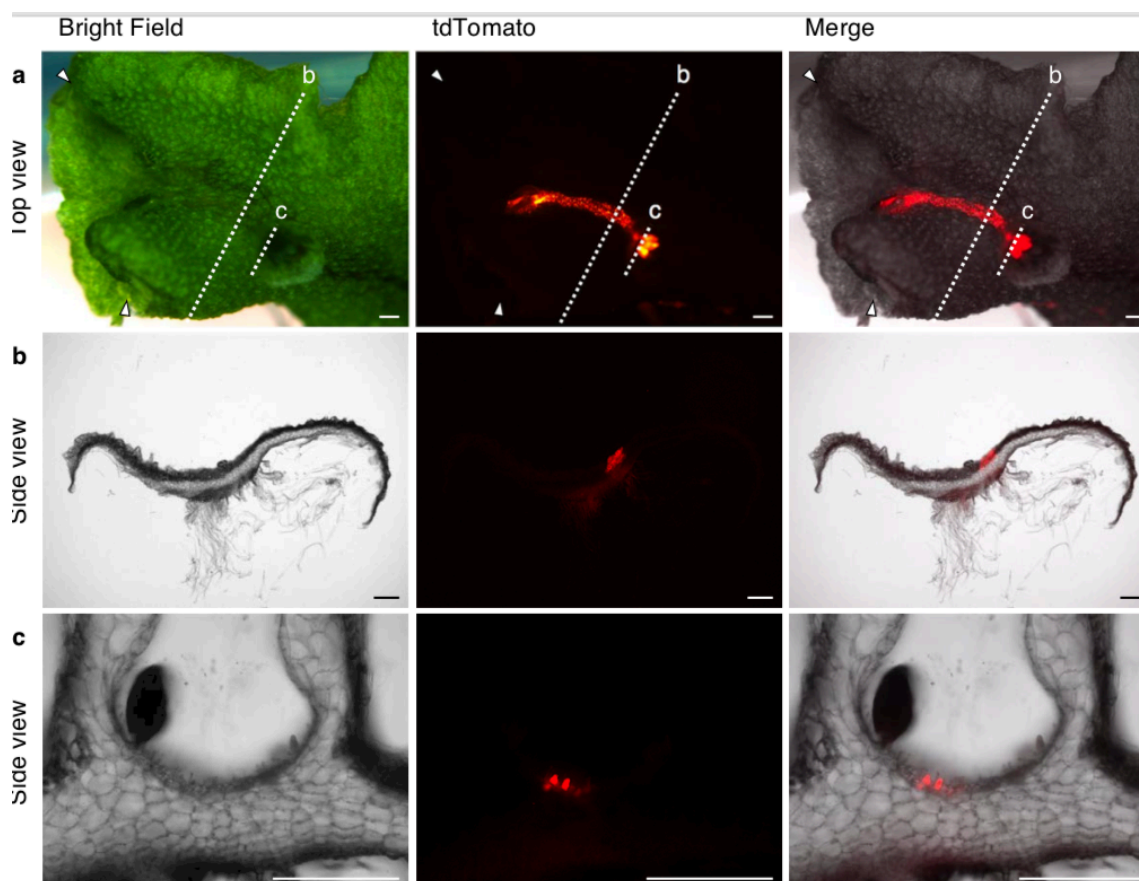
484

485



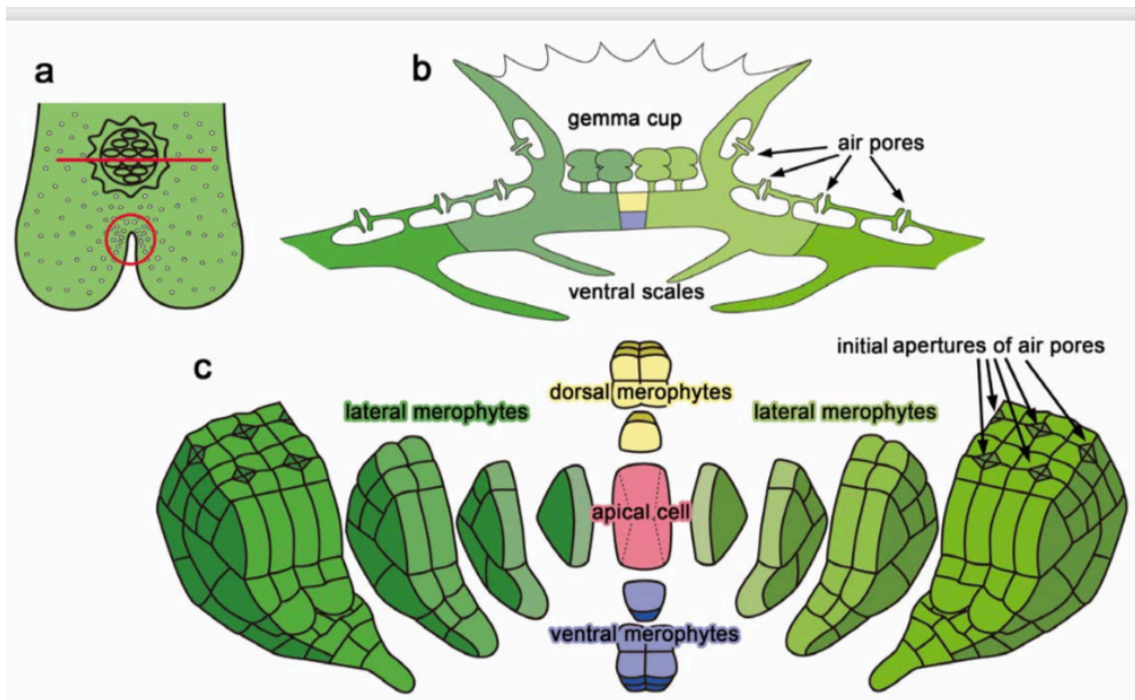
486 **Fig. 5** Division of gemma cups by thallus-bisecting sectors

487 **a** Correlation between gemma cup positions and plastochron numbers. Circles and
488 differently coloured lines indicate gemma cups and the growth phase of each plastochron,
489 respectively. Gemma cups were never formed during the 1st plastochron under the growth
490 conditions we used. **b** A gemma cup bisected by a merophyte sector. A white dotted line
491 in the merged picture indicates an outline of the gemma cup. Scale bars = 500 μ m. **c**
492 Vertical transverse section of a gemma cup on a merophyte sector. Scale bars = 500 μ m.
493 **d** Dot- and box-plots for the ratio of tdTomato-positive serration edges in a gemma cup
494 formed on a thallus-bisecting sector. The dots are individual values. The bottom and top
495 of each box represent the first and third quartiles, respectively. The band inside the box is
496 the median.



497 **Fig. 6** Division of gemma cups by dorsal merophyte sectors

498 **a–c** Top (**a**) and side (**b** and **c**) views of a dorsal line-shaped sector along the midrib that
 499 includes a part of gemma cup in the third plastochron of a 23-day-old plant. Scale bars =
 500 500 μm . White dotted lines in **a** indicate the approximate positions of the side-view
 501 sections in **b** and **c** (basal sides observed). Arrowheads in **a** indicate apical notches.
 502



503

504 **Fig. 7** Models of dorsal organ formation in relation to merophytes

505 Red line and circle in **a** indicate the positions of schematic illustrations for a gemma cup
 506 part (vertical transverse section, **b**) and the notch (front view, **c**). Cells in red, yellow,
 507 purple, and different levels of green colors in **b** and **c** indicate an apical cell, dorsal
 508 merophytes, ventral merophytes, and lateral merophytes, respectively.

509